

# CrystEngComm

Accepted Manuscript



This is an *Accepted Manuscript*, which has been through the Royal Society of Chemistry peer review process and has been accepted for publication.

*Accepted Manuscripts* are published online shortly after acceptance, before technical editing, formatting and proof reading. Using this free service, authors can make their results available to the community, in citable form, before we publish the edited article. We will replace this *Accepted Manuscript* with the edited and formatted *Advance Article* as soon as it is available.

You can find more information about *Accepted Manuscripts* in the [Information for Authors](#).

Please note that technical editing may introduce minor changes to the text and/or graphics, which may alter content. The journal's standard [Terms & Conditions](#) and the [Ethical guidelines](#) still apply. In no event shall the Royal Society of Chemistry be held responsible for any errors or omissions in this *Accepted Manuscript* or any consequences arising from the use of any information it contains.



Journal Name

COMMUNICATION

## Magneto-acceleration of Ostwald Ripening in Hollow Fe<sub>3</sub>O<sub>4</sub> Nanospheres

Received 00th January 20xx,  
Accepted 00th January 20xx

Wei Ding,<sup>i,ab</sup> Lin Hu,<sup>i,c</sup> Zhigao Sheng,<sup>\*cd</sup> Jianming Dai,<sup>\*a</sup> Xuebin Zhu,<sup>a</sup>

DOI: 10.1039/x0xx00000x

Xianwu Tang,<sup>a</sup> Zhenzhen Hui,<sup>a</sup> and Yuping Sun<sup>acd</sup>

www.rsc.org/

**The magnetic field induced acceleration of Ostwald ripening process was demonstrated firstly in the formation of hollow Fe<sub>3</sub>O<sub>4</sub> nanospheres. As well as maintaining time, the magnetic field can act as an independent parameter to control the crystallite size, hollow structure, and pore size of nanostructure in the Ostwald ripening process.**

Ostwald ripening, as a description for the coarsening and secondary re-crystallization process, was firstly discovered by Friedrich Wilhelm Ostwald in 1900.<sup>1</sup> It has been observed in crystal growth for more than one century and plays an important role in catalyst sintering.<sup>2</sup> Recently, the design and fabrication of hollow and porous nanostructure have attracted much attention in materials research because of their enhanced properties in the fields of catalysis,<sup>3</sup> sensing,<sup>4</sup> energy storage,<sup>5,6</sup> photoactivity,<sup>7</sup> and drug delivery<sup>8</sup> owing to their large specific surface area and hollow interior space. Ostwald ripening, as a century-old phenomenon, provides a newer self-template plate based method for the preparation of the hollow and porous nanostructures in addition to the templating synthesis methods. For example, Zeng et al. used Ostwald ripening as a template-free route to prepare anatase TiO<sub>2</sub> hollow spheres in 2004.<sup>9</sup> Their subsequent works have also demonstrated that the Ostwald ripening can indeed as a general mechanism for fabrication the hollow spheres of metal oxides and sulfides in solution.<sup>10-13</sup> Nowadays, Ostwald ripening has been proven as an effective synthetic strategy for the formation of interior spaces in hollow spherical and nonspherical structures of

CoFe<sub>2</sub>O<sub>4</sub>,<sup>14</sup> α-MnO<sub>2</sub>,<sup>15</sup> SnO<sub>2</sub>,<sup>6</sup> γ-MnS,<sup>16</sup> CaTiO<sub>3</sub>,<sup>17</sup> etc.

Ostwald ripening has become a sophisticated approach for making highly complex nanostructures, but its complex matter's relocation mechanism and artificial modulating have been rarely explored, though it is the basis for the controllable materials architecture in this field. Recent years, people have done a number of related attempts. For example, it was discovered that this ripening process can be promoted specifically by fluoride-mediated surface dissolution in synthesis process of TiO<sub>2</sub> and SnO<sub>2</sub> hollow microspheres.<sup>18</sup> In 2011, Wang et al. found that the longer maintaining time and higher reaction temperature can apparently favor matter relocation in ripening process in the experiment of preparation of SiO<sub>2</sub> hollow spheres.<sup>13</sup> As an important thermodynamic factor, magnetic field can affect the physical and chemical process of material in a non-contact form and has been introduced in the synthesis process to control the nanostructure.<sup>19-22</sup> However, up to now, the nanostructure fabrication using Ostwald ripening in a magnetic field and the magneto-effect on ripening process has not been touched. In this study, we take mesoporous Fe<sub>3</sub>O<sub>4</sub> as an example to demonstrate the effect of magnetic fields on Ostwald ripening process for the first time. The acceleration of Ostwald ripening caused by magnetic fields was found in the preparation of hollow-mesoporous Fe<sub>3</sub>O<sub>4</sub> nanospheres.

Fe<sub>3</sub>O<sub>4</sub> nanospheres were prepared by the solvothermal method. The products are denoted by S10h-0T, S24h-0T, S48h-0T, S10h-0.5T,

<sup>a</sup>Key Laboratory of Materials Physics, Institute of Solid State Physics, Chinese Academy of Sciences, Hefei 230031, People's Republic of China.

<sup>b</sup>University of Science and Technology of China, Hefei 230026, People's Republic of China.

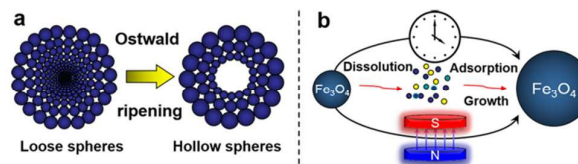
<sup>c</sup>High Magnetic Field Laboratory, Chinese Academy of Sciences, Hefei 230031, People's Republic of China.

<sup>d</sup>Collaborative Innovation Centre of Advanced Microstructures, Nanjing University, Nanjing 210093, People's Republic of China.

†Electronic Supplementary Information (ESI) available: Detailed experimental procedures; XRD patterns, FE-SEM images, and magnetization of Fe<sub>3</sub>O<sub>4</sub> nanospheres. See DOI: 10.1039/x0xx00000x

\*W. D. and L. H. contributed equally to this work.

This journal is © The Royal Society of Chemistry 20xx



Scheme 1. The schematic illustration of Ostwald ripening process (a) and its magneto-acceleration effect (b).

S10h-1T and S10h-3T, respectively, according to the maintaining time and applied magnetic fields (see Supporting Information).

The powder X-ray diffraction (XRD) patterns confirm that all samples are well crystallized and no other phase is detectable (Figure S1 and S2). The field emission scanning electron microscopic (FE-SEM) images, shown in Figure 1, verified that all the samples have spherical shape with a homogeneous diameter of  $\sim 250$  nm (Figure S3). The shell of nanospheres consists of a loosely packed aggregating of  $\text{Fe}_3\text{O}_4$  nanoparticles and the size of those nanoparticles increases gradually with the increase of maintaining time (Figure 1a-1c). This is the typical feature of Ostwald ripening. With application of magnetic fields, it is interesting to find that the  $\text{Fe}_3\text{O}_4$  nanoparticle size is enlarged with the magnetic field intensity increasing though the same time (10 h) was maintained (Figure 1a and Figure 1d-1f).

To determine the size dispersion in detail, the size distribution of the  $\text{Fe}_3\text{O}_4$  nanoparticles was estimated by taking the average size of 150 nanoparticles and fitting the resultant histogram by a Gaussian function (dotted lines). The typical results have been shown in the Figure 1g and 1h. It was found that the central size was shifted from 27.2 to 48.8 nm and 27.2 to 44.0 nm as maintaining time was prolonged from 10 to 48 h and magnetic field was increased from 0 to 1T, respectively. These results clearly confirmed that the effect of magnetic field on the particle-size of the mesoporous  $\text{Fe}_3\text{O}_4$  spheres is similar to that of maintaining time. In particular, the morphology of S10h-0.5T is similar to that of S24h-0T, and the morphology of S10h-1T is similar to that of S48h-0T. When magnetic field exceeds 1T, the particle size expands slowly. For instance, the particle size increases only 2.5% (from 44.0 to 45.1 nm) when the magnetic field was enhanced from 1 to 3 T, which implies that Ostwald ripening effect tends to be saturated in this case when the magnetic field beyond 1 T.

In Ostwald ripening process, a "solid-solution-solid" mass transportation happens (Scheme 1). The  $\text{Fe}_3\text{O}_4$  crystallites located in the outermost surface are larger and would grow at the expense of smaller ones inside through the transportation as shown in Scheme 1.<sup>10, 23</sup> Consequently, such gradual outward migration of crystals

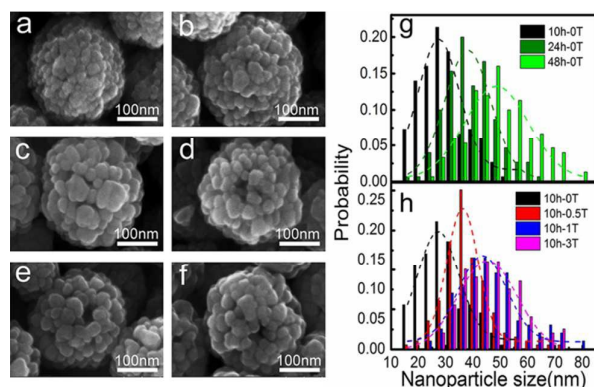


Figure 1. FE-SEM images of: S10h-0T (a); S24h-0T (b); S48h-0T (c); S10h-0.5T (d); S10h-1T (e); S10h-3T (f); and histogram of particle-size distribution for the hollow nanospheres prepared without (g) and with (h) magnetic fields.

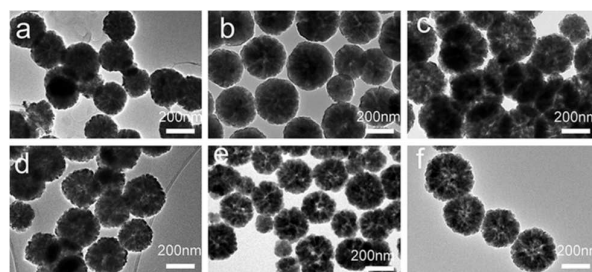


Figure 2. TEM images of: S10h-0T (a); S24h-0T (b); S48h-0T (c); S10h-0.5T (d); S10h-1T (e) and S10h-3T (f).

would result in continuing expansion of interiorly void space within the nanospheres. The evolutionary steps of interior spaces for  $\text{Fe}_3\text{O}_4$  spheres in our case were studied by transmission electron microscopy (TEM) as shown in Figure 2, S4 and S5. The S10h-0T sample shows a solid sphere structure with straight channel-like mesoporous directly access to the center of the sphere (Figure 2a). With increasing of maintaining time, the S24h-0T displays a star-shaped void space at the center of the sphere, and the straight channel-like mesoporous become larger compared to that of the S10h-0T (Figure 2b). With time increasing further, the void spaces at the center of the spheres in the S48h-0T become larger (Figure 2c). With application of magnetic fields, an obvious expansion of void space was also found under the same maintaining time. Different from the solid sphere structure of S10h-0T sample, a small void space starts to form at the center of the sphere in the S10h-0.5T (Figure 2d) and it becomes larger with the increase of magnetic field intensity (Figure 2e and 2f). Furthermore, we note that the hollow structure of S10h-0.5T is nearly the same as that of S24h-0T, while the hollow structure of the S10h-1T is also similar to that of the S48h-0T.

In order to verify the magneto-acceleration effect further, the mesoporous size distribution of  $\text{Fe}_3\text{O}_4$  nanospheres were measured

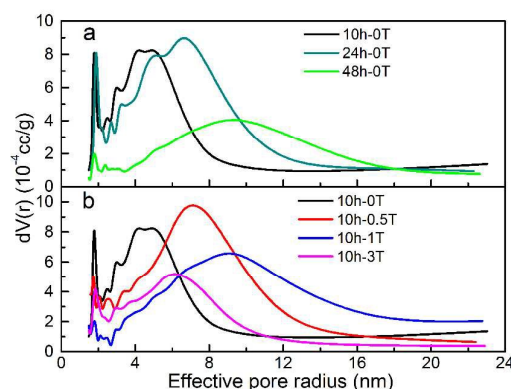


Figure 3. Pore-size distribution curve of hollow  $\text{Fe}_3\text{O}_4$  spheres obtained without (a) and with (b) magnetic fields.

by Barrett Joyner Halenda (BJH) methods and the typical results were displayed in Figure 3. The peak values of the pore size increase gradually from 4.6 to 6.7 and 9.2 nm when the maintaining time prolongs from 10 to 24 and 48 h, respectively. Similarly, the peak values of the pore size distribution of the S10h-0.5T and S10h-1T are found as 7.1 and 9.1 nm, respectively. This magneto-enhancement of pore size of Fe<sub>3</sub>O<sub>4</sub> nanospheres, together with XRD, FE-SEM, and TEM results, suggest that the external magnetic field can significantly accelerate the Ostwald ripening process. When the external magnetic field exceeds the saturation value 1 T, it is interesting to find that the pore size shrinks and it was reduced down to 6.1 nm under the magnetic field of 3 T. This probably because the significant enhancement of mutually magnetic attraction between Fe<sub>3</sub>O<sub>4</sub> particles in the higher magnetic field.

In the Ostwald ripening process, the Fe<sub>3</sub>O<sub>4</sub> particles located in the outermost surface of aggregates grow at the expense of smaller ones inside, due to the higher solubility of the smaller particles (Gibbs-Thomson or Kelvin effect) and the molecular diffusion through the continuous phase (Scheme 1b).<sup>24</sup> Gradual melting and outward migration of the inside particles would lead to continuing expansion of interior space (Scheme 1). With application of magnetic field, two aspects should be addressed. At first, the applied magnetic field will produce a magnetic energy  $E_M = -\chi V H^2 / 2\mu_0$ , in which  $\mu_0$  is the permeability of free space,  $\chi$  is the volume magnetic susceptibility, V is the volume of Fe<sub>3</sub>O<sub>4</sub> particles here, H is magnetic field intensity. The negative magnetic energy  $E_M$  plays a crucial role in the surface energy reduction of nanoparticles. Then, the larger Fe<sub>3</sub>O<sub>4</sub> particles at outermost surface, which owning large  $E_M$  and less surface energy, would be easier to produce in the ripening process.<sup>20</sup> On the other hand, the participation of external magnetic field will also affect the free energy ( $\Delta G$ ) of ripening process directly. In addition to the original thermal Gibbs free energy  $\Delta G_T(T)$ , the magnetic Gibbs free energy  $\Delta G_M(T, H)$  should be considered and the total Gibbs free energy of the ripening process  $\Delta G = \Delta G_T + \Delta G_M$ .<sup>25</sup> The  $\Delta G_M(T, H)$  can be written as  $-\mu_0(\chi_a - \chi_b)H^2/2$ , in which  $\chi_a$  and  $\chi_b$  are the volume magnetic susceptibility of the magnetic particles after and before ripening, respectively. The smaller Fe<sub>3</sub>O<sub>4</sub> nanoparticles, with diameter less than 30 nm in our case, are very close to the size limitation of superparamagnetic state (~20 nm) and produce a negligible susceptibility  $\chi_b$ .<sup>26</sup> In the ripening process, the size enlargement of Fe<sub>3</sub>O<sub>4</sub> nanoparticles favors for the stabilization of ferromagnetic phase and a larger  $\chi_a$ . The magnetization measurement of these Fe<sub>3</sub>O<sub>4</sub> nanospheres indicates that the sample with larger particles has larger saturation magnetization (Figure S6). Consequently, the negative  $\Delta G_M$  is suggested and it contributes such magneto-acceleration of Ostwald ripening according to the theory that the state variation of the material advances toward the direction where the free energy is the lowest.<sup>27</sup> To clarify the intrinsic mechanism of magnetic field effect, theoretical calculation and further experiments on such issue should be done in the future.

## Conclusions

In summary, we report the magnetic field induced acceleration of Ostwald ripening in Fe<sub>3</sub>O<sub>4</sub> nanospheres for the first time. As an

independent parameter, the external magnetic field are found to be an alternative tool to control the crystallite size, hollow structure, and pore diameter of the mesoporous Fe<sub>3</sub>O<sub>4</sub> nanostructures. Reduction of surface energy of nanospheres and negative magnetic free energy caused by external magnetic field were discussed for the explaining of such acceleration effect. Our results suggest that the magnetic field can be a novel approach to control the fabrication of hollow and porous nanostructures with the advantages of a simple yet very efficient and contact-free, which might be very useful for future technological applications.

## Acknowledgment

We gratefully acknowledge financial support from the National Science Foundation of China (NSFC; Grant Nos. U1232210, 11574316, U1532155, 21301178) the National Key Basic Research Project of China (grant No. 2014CB931704), and the One Thousand Youth Talents Program of China.

## Notes and references

- 1 W. Z. Ostwald, *Phys. Chem.*, 1900, 34, 495–503.
- 2 P. Wynblatt and N. A. Gjostein, *Prog. Solid. State. Chem.*, 1975, 9, 21.
- 3 R. T. Dong, H. L. Wang, Q. Zhang, X. T. Xu, F. Wang and B. Li, *CrystEngComm*, 2015, 17, 7406–7413.
- 4 D. W. Wang, S. S. Du, X. Zhou, B. Wang, J. Ma, P. Sun, Y. F. Sun and G. Y. Lu, *CrystEngComm*, 2013, 15, 7438–7442.
- 5 L. Y. Dang, H. F. Ma, J. Y. Xu, Y. Jin, J. J. Wang, Q. Y. Lu and F. Gao, *CrystEngComm*, 2016, 18, 544–549.
- 6 X. W. Lou, Y. Wang, C. L. Yuan, J. Y. Lee and L. A. Archer, *Adv. Mater.* 2006, 18, 2325–2329.
- 7 P. W. Li, X. L. Yan, Z. Q. He, J. L. Ji, J. Hu, G. Li, K. Lian and W. D. Zhang, *CrystEngComm*, 2016, 18, 1752–1759.
- 8 R. C. Lv, S. L. Gai, Y. L. Dai, F. He, N. Niu and P. P. Yang, *Inorg. Chem.* 2014, 53, 998–1008.
- 9 H. G. Yang and H. C. Zeng, *J. Phys. Chem. B.*, 2004, 108, 3492–3495.
- 10 J. Li and H. C. Zeng, *J. Am. Chem. Soc.*, 2007, 129, 15839–15847.
- 11 Y. Chang, J. J. Teo and H. C. Zeng, *Langmuir.*, 2005, 21, 1074–1079.
- 12 B. Liu and H. C. Zeng, *Small*, 2005, 1, No. 5, 566–571.
- 13 D. P. Wang and H. C. Zeng, *Chem. Mater.*, 2011, 23, 4886–4899.
- 14 H. Zhang, C. Zhai, J. Wu, X. Ma and D. Yang, *Chem. Commun.* 2008, 5648–5650.
- 15 B. X. Li, G. X. Rong, Y. Xie, L. F. Huang and C. Q. Feng, *Inorg. Chem.*, 2006, 45, 6404–6410.
- 16 Y. H. Zheng, Y. Cheng, Y. S. Wang, L. H. Zhou, F. Bao and C. Jia, *J. Phys. Chem. B.*, 2006, 110, 8284–8288.
- 17 X. F. Yang, J. X. Fu, C. J. Jin, J. Chen, C. L. Liang, M. M. Wu and W. Z. Zhou, *J. Am. Chem. Soc.*, 2010, 132, 14279–14287.
- 18 J. G. Yu, H. T. Guo, S. A. Davis and S. Mann, *Adv. Funct. Mater.*, 2006, 16, 2035–2041.
- 19 Y. Ikezoe, N. Hirota, J. Nakagawa, and K. Kitazawa, *Nature*, 1998, 393, 750.
- 20 J. Wang, Q. W. Chen, C. Zeng and B. Y. Hou, *Adv. Mater.*, 2004, 16, 137–140.
- 21 L. Hu, R. R. Zhang and Q. W. Chen, *Nanoscale*, 2014, 6, 14064.
- 22 K. J. Zhang, J. M. Dai, X. B. Zhu, X. G. Zhu, X. Z. Zuo, P. Zhang, L. Hu, W. J. Lu, W. H. Song, Z. G. Sheng, W. B. Wu, Y. P. Sun and Y. W. Du, *Scientific Reports*, 2016, 6, 19483.
- 23 C. Y. Christopher and H. C. Zeng *J. Mater. Chem. A*, 2014, 2, 4843–4851

## COMMUNICATION

Journal Name

- 24 Y. De Smet, L. Deriemaeker and R. Finsy, *Langmuir*, 1999, 15, 6745-6754.
- 25 J. H. Wang, Y. W. Ma and K. Watanabe, *Chem. Mater.*, 2008, 20, 20-22.
- 26 C. J. Xu and S. H. Sun, *Advanced Drug Delivery Reviews*, 2013, 65, 732-743.
- 27 K. Ichikawa, and S. Shiratori, *Inorg. Chem.*, 2011, 50, 999-1004.